17th World Conference on Earthquake Engineering, 17WCEE
Sendai, Japan - September 13th to 18th 2020

ISOLATION RISK ANALYSIS IN MOUNTAINOUS AREA CONSIDERING EARTHQUAKE-INDUCED SLOPE FAILURES

Y. Ono [1], K. Hibi [2]

[1] *Professor, Tottori University, ysk@tottori-u.ac.jp*
[2] *Graduate student, Tottori University, m18j6028c@edu.tottori-u.ac.jp*

Abstract

The aim of this paper is to present a methodology to assess the isolation risk of residents in mountainous areas considering earthquake-induced slope failures. After the 2004 Niigata Chuetsu earthquake, most residents in Yamakoshi village were isolated due to the blockage of the road network. As a result, they were forced to leave their home at least for several months. The disaster arose a social interest in the isolation in mountainous areas in Japan. For preventing isolation in a mountainous area, the first step is to identify areas that have high isolation risk. In this study, we present a methodology to evaluate the isolation risk based on the probability of isolation and population data. The following procedure is utilized. First, the probabilities of slope failures in the study area are calculated using slope gradient and PGA distribution. The slope gradient is calculated from the digital elevation model (DEM). The PGA distribution is converted from the JMA seismic intensity map for a scenario earthquake published by Japan Seismic Hazard Information Station (J-SHIS). Second, the road network is modeled as a graph consisting of nodes and edges, and the probabilities of node and edge failures are computed according to the probability of slope failures obtained in the previous step. Third, the probability of isolation from each node to the town hall, where the headquarters of emergency response would be placed, is calculated by the Monte-Carlo (MC) method. Finally, the expected number of the isolated residents allocated to each node is calculated as an index of isolation risk. We applied the presented methodology to Chizu Town, Tottori, Japan, as a case study. Chizu Town is a typical rural town in Japan and suffers from a rapid decline and aging of its population. The probabilities of isolation and the expected number of the isolated residents in the town considering an *Mw* 6.8 scenario earthquake published by J-SHIS are presented. The road network was modeled as a graph with 1,134 nodes and 1,475 edges. The results presented in this study enable the authorities and the stakeholders, who are responsible for earthquake disaster mitigation, to perform reinforcement of the road network efficiently and to develop the emergency response plan in the study area.

Keywords: Isolation; Slope failure; Road blockage; Network analysis; Mountainous area; Chizu Town

1. Introduction

Road blockages induced by slope failures during an earthquake cause significant functional loss to traffic networks. Especially when a destructive earthquake ground motion strikes a mountainous area, residents are prone to be isolated due to road blockage. Once isolated, the residents suffer from difficulties not only in emergency rescue and aid operations but also in daily lives for the long term. During the 2004 Niigata Chuetsu Earthquake, a vast number of slope failures occurred in Yamakoshi Village, which is currently a part of Nagaoka City, and after the earthquake, most residents in the village were isolated. In addition, the 2016 Kumamoto earthquake caused many slope failures and resulted in the isolation of several parts of Minami-Aso Village. Based on these experiences, social interest in the development of effective countermeasures to the isolation of residents in mountainous areas has increased.

In developing the isolation countermeasures for residents in mountainous areas, it is necessary to evaluate their risks quantitatively. Isolation of residents can be analyzed as a connectivity problem of a road network. Numerous studies [1–6] have been conducted on the connectivity of road networks, considering earthquake hazards. In urban road networks, road blockage generally caused by damage to structures and traffic congestions are primary concerns. However, in the case of a mountainous road network, slope failures are more likely to induce road blockages rather than damage of structures, and traffic concentration will not occur. Furthermore, compared to urban areas, the number of alternative routes is limited, and network isolation is likely to take place in mountainous areas. As far as the authors know, the isolation risk of residents in mountainous areas under a seismic hazard has been rarely studied. Michael-Leiba et al. [7] mentioned the isolation risk of communities considering landslide, but no quantitative analysis was conducted.

The objective of this study is to present a methodology to analyze the isolation risk of residents in mountainous areas after a destructive earthquake based on the connectivity analysis used for road networks in urban areas. Although road blockage can take place due to damage to bridges, tunnels, and other structures, the slope failures induced by earthquake ground motions are considered in this study. The isolation risk of residents is quantified as the probability of isolation and the expected values of isolated people.

Section 2 describes a method to estimate the isolation risk of residents considering road blockage induced by slope failures during an earthquake and the data used in this study. Sections 3 and 4 show a case study in which the presented method is applied to Chizu Town, Tottori, Japan. This case study reveals the distribution of isolation risk during an earthquake in the town. Section 5 concludes the study.

2. Data and Methodology

In this study, the isolation risk of residents in a mountainous area is analyzed in four steps: (1) estimation of the probability of slope failure; (2) estimation of the probability of node and edge failure; (3) estimation of the probability of isolation; (4) estimation of the expected number of isolated residents. The following describes each of these steps. The datasets required to perform the analysis are the digital elevation model (DEM), the intensity of earthquake ground motion, the graph of the road network, and the population distribution in the study area. The procedure and flow of the input data are summarized in Fig. 1.

2.1 Probability of slope failure

We used the equation developed by Sakai et al. [8] to calculate the probability of slope failure. The probability of slope failure is defined as a probability of occurrence of at least one slope failure in a 10 m grid cell, and the scale of the slope failure or the number of slope failures in a cell is not considered. According to Sakai et al.[8], the probability of slope failure P^f_s is given by the following equation using the slope gradient ϕ (deg.) and the peak ground acceleration (PGA) a (cm/s^2).

$$P_s^f = \frac{1}{1+\exp\{-\ -7.89+0.09\phi+0.0019a\ \}} \tag{1}$$

where ϕ is the slope gradient. In this study, ϕ was obtained from digital elevation models (DEM) using GIS software. The DEM data of a 10 m spatial resolution published by the Geospatial Information Authority of Japan (GSI) was used. The PGA values were obtained from the ground motion prediction map published by Japan Seismic Hazard Information Station (J-SHIS) operated by the National Research Institute for Earth Science and Disaster (NIED). The ground motion prediction map published by J-SHIS shows the spatial distribution of ground motion when a specific fault is activated. However, although the spatial distribution of the JMA seismic intensity scale (SI) and the peak ground velocity (PGV) are given, that of the PGA is not available. Therefore, we converted SI to PGA by the following equation developed by Fujimoto and Midorikawa [9];

$$SI = -0.122 + 0.114\ M_w + 1.682\ \log\ (a) + 0.069 \log\ a^2 \tag{2}$$

where M_w and a denotes the moment magnitude and PGA, respectively. From Eq. (2), we obtain,

$$a = 10^{\frac{\sqrt{-7866M_w L69000SIL715699} - 841}{69}} \tag{3}$$

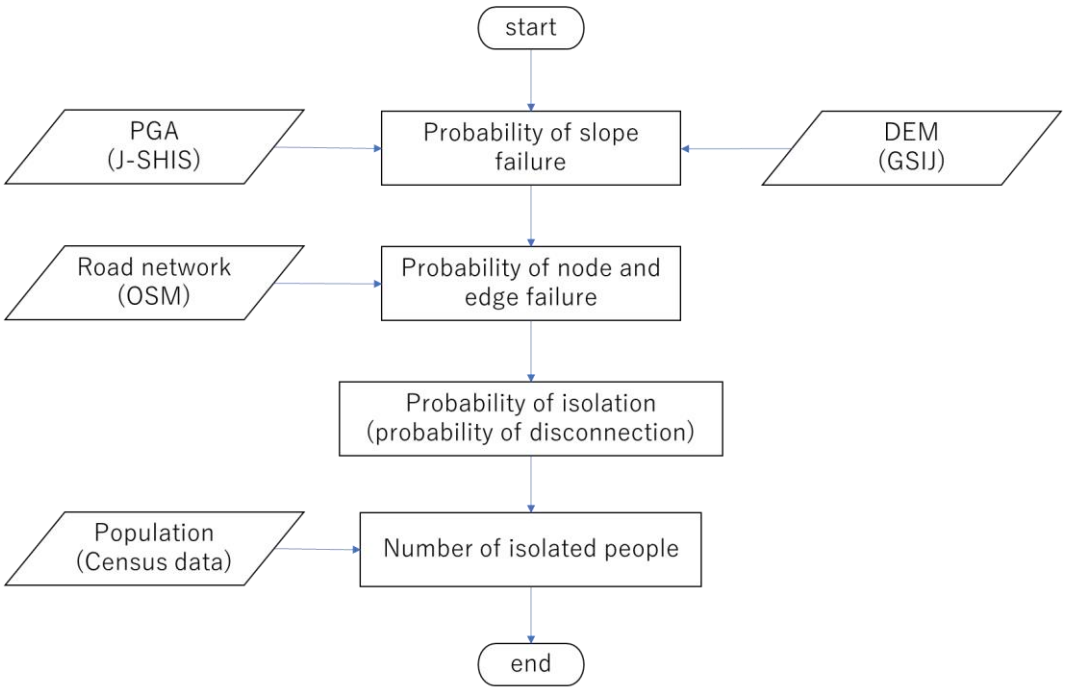

Fig. 1 – Flowchart of calculating probabilities of node isolation and the number of isolated people

2.2 Probability of node and edge failure

The road network data was downloaded from OpenStreetMap [10] and saved as the line vector data in the GIS shapefile format. The line vector data of the road network were converted to a graph consists of nodes and edges by use of OSMnx library [11] in Python programming language. A node represents an intersection or a terminal point of the road while an edge connects a pair of nodes.

It is assumed that node failure is caused by the slope failure at the location of the node. Therefore, the failure probability of a node is obtained by referring to the value of the slope failure probability at the position in the raster data.

On the other hand, it is defined that an edge fails when at least one slope failure occurs in the edge. To obtain the failure probability of an edge, we generate evaluation points in the edge, as shown in Fig.2. These

evaluation points are generated one by one for all the slope failure probability raster cells that overlap with the edge. Then the failure probability of the edge *i* is calculated by the following equation.

$$P_i^f = 1 - \prod_{j=1}^{n}(1 - p_j^f) \tag{4}$$

where P^f_j denotes the probability of slope failure at the evaluation point *j*, and *n* is the number of evaluation points generated in the edge. The evaluation points located in the same cell as the nodes of the edge are ignored because the probabilities of slope failure in these cells are considered in the evaluation of the probabilities of node failure.

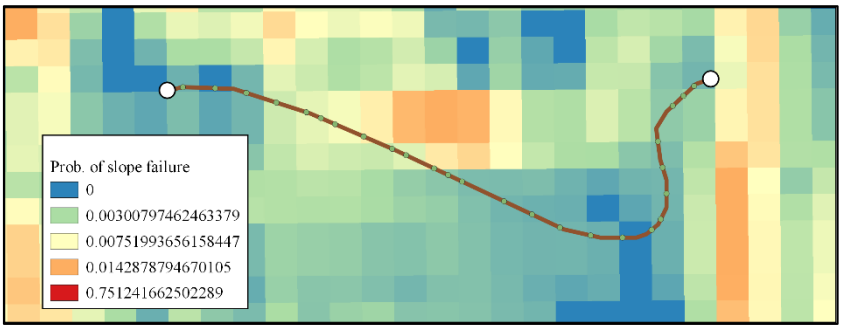

Fig. 2 – Generated evaluation points on an edge and raster data cells showing the probabilities of slope failure

2.3 Probability of isolation

In this study, isolation of residents is defined as a state in which no path between the nearest node of the residents and the destination node corresponding to the town hall, where disaster management headquarters office will be placed. The isolation probability of residents is given as the probability of disconnection between the nearest node of the residents and the node corresponding to the town hall. To calculate the probability of isolation, we conduct the analysis on the probability of connection based on graph theory. Numerous algorithms to compute the probability of network connection: enumerating methods [12–14], decomposition methods [15,16], Monte-Carlo (MC) methods [17–19], and et al. In this study, the MC method was applied since it is easy to be implemented in the computer code and is efficient in computation for a large-scale network.

The P^I_j, the isolation probability of the node *j* is given by,

$$P_j^I = 1 - P_j^C \tag{5}$$

where P_i^C is the probability of a connection between node *j* and the destination node. We calculate the isolation probability for all nodes except the destination node. The computer code to calculate the isolation probability was developed by the authors using Python language with NetworkX library [20].

2.4 Expected number of the isolated residents

The expected number of the isolated residents is used as an index to represent the isolation risk and is evaluated for each node. Let denote the expected number of the isolated residents of node *j* by $E(N_j)$, and it is given by,

$$E(N_j) = P_j^I N_j \tag{6}$$

where N_j is the population assigned to node *j*, and P^I_j is the isolation probability of node *j*.

To allocate N_j to node *j*, we use the national census data published by the Japanese Bureau of Statics. The census data is provided in the GIS shapefile format. The census data are defined for each ward, which is

a small administrative section in a city, town, or village. We allocate equivalently the population for one ward defined in the census data to nodes in the ward. Thus, the population assigned to node *j*, N_j, is given by,

$$N_j = \frac{N}{n} \tag{7}$$

where *N* is the total population, and *n* is the number of nodes in the ward.

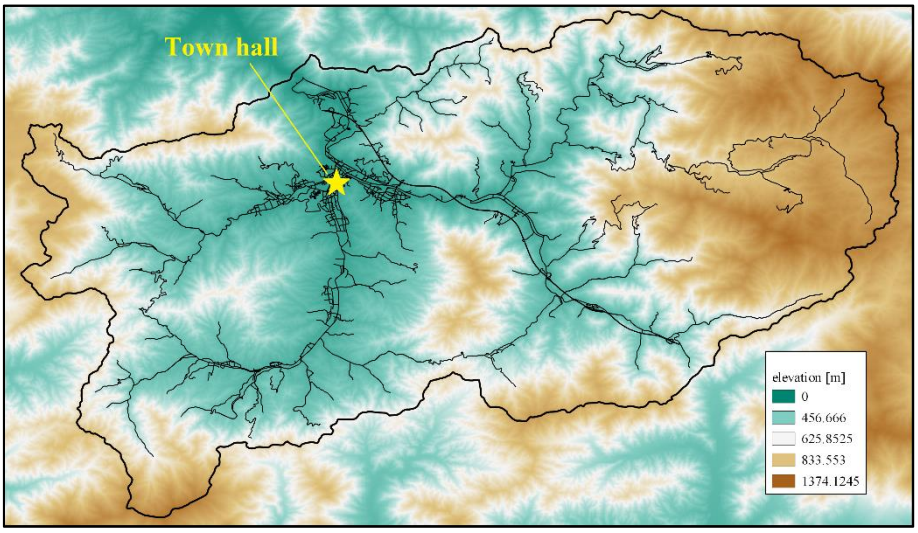

Fig. 3 – Topography and road network of Chizu town, Tottori, Japan

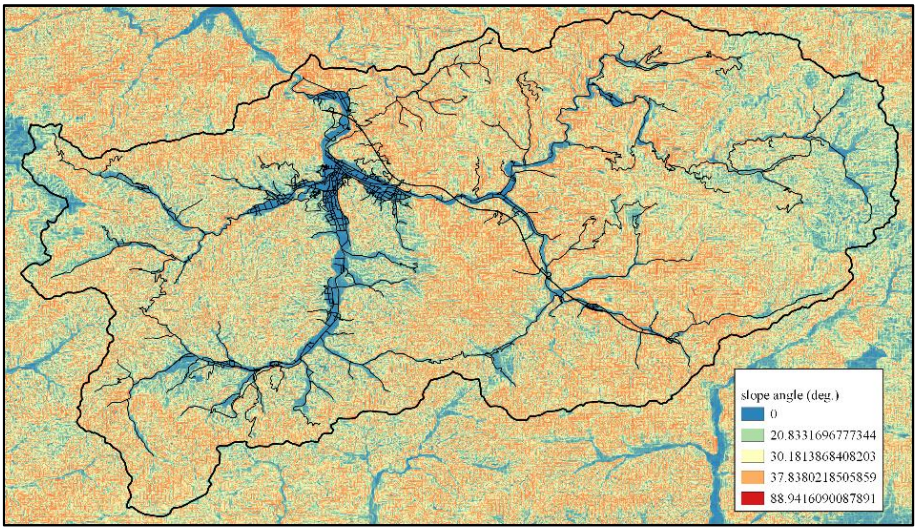

Fig. 4 – Slope gradient (deg.)

3. Study area

Chizu Town, Tottori, Japan, is one of the typical rural towns in a mountainous area in Japan. More than 90% of the town is forested. The population of the town is about 6,500 in 2020, but it is declining and aging rapidly. Declining and aging of the population are common problems in mountainous areas of Japan.

The topography of Chizu Town is shown in Fig. 3. The political boundary of the town is represented by the thick solid line. Most of Chizu Town is located higher than 450 m from the sea level. In the same figure,

the road network of the town is drawn by the thin solid lines. The central part of the town is placed on the lower flat land, and the road network spreads to higher places. In this study, we assumed that a disaster management headquarters would be placed in the town hall. Therefore, the isolation probability of each node on the road network equals to the disconnection probability from the node to the town hall. In Fig.3, the location of the town hall is shown. The graph of the road network used in this study consists of 1,134 nodes and 1,475 edges.

On the other hand, Fig. 4 shows the slope gradients in Chizu Town. Some parts of the road network run through the steep slope area, although most of the road network is placed on the flat land.

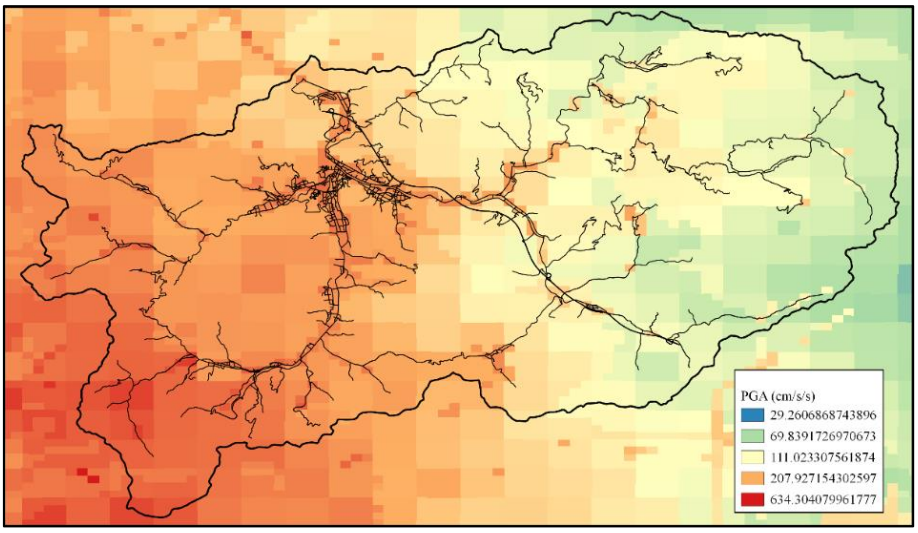

Fig. 5 – PGA (downloaded from J-SHIS)

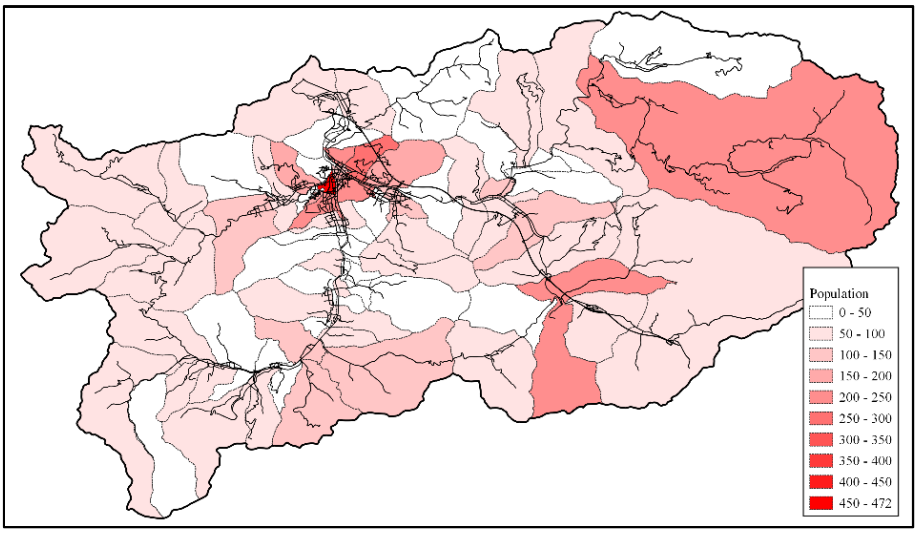

Fig. 6– Population distribution

To calculate the probability of slope failure, we used a scenario earthquake shaking map published by J-SHIS. J-SHIS has released scenario earthquake shaking maps for major active faults in Japan as well as the probabilistic seismic hazard maps. In J-SHIS's shaking maps, ground motion intensity is given by JMA seismic

intensity (SI) and peak ground velocity (PGV). We converted SI to PGA by means of Eq. (3). In this study, we used the event of *Mw* 6.8 in the Nagisan fault zone, which gives the most significant scenario for Chizu Town.

Figure 5 shows the distribution of the converted PGA. The source fault is placed in the west of Chizu Town, and the western part of the town is shaken stronger than the eastern part is. The maximum value of PGA in Chizu Town is approximately 640 cm/s^2, while the minimum value is lower than 100 cm/s^2. Since the spatial resolution of the raster data provided by J-SHIS is 200 m, we interpolated the PGA map to a spatial resolution of 10 m before calculating the probability of slope failure.

The population distribution in Chizu Town is shown in Fig. 6. The wards near the town hall have the largest population. There are wards with a large population even in the wards on the town border from the town hall. The road network in the wards near the town hall is dense, while the road network in the wards near the town border is sparse.

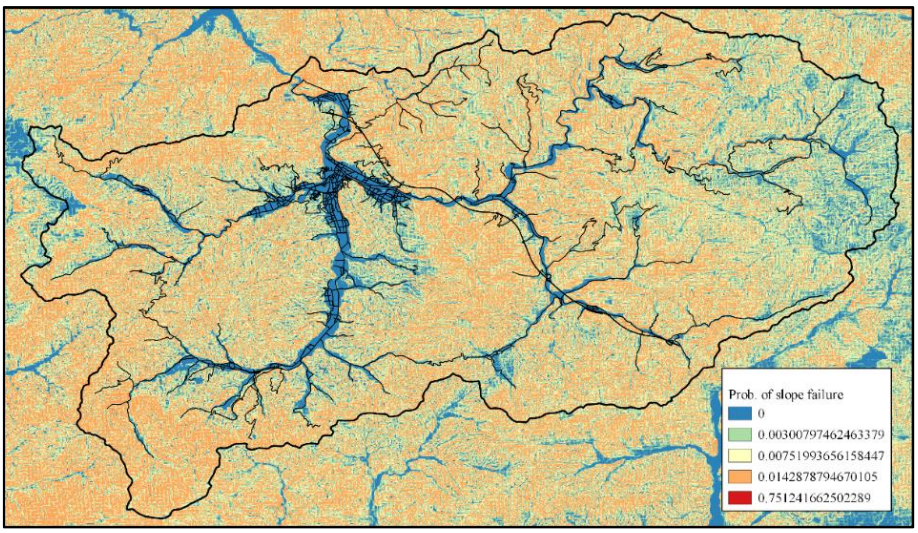

Fig. 7 – Probability of slope failure

4. Results and discussion

4.1 Probability of slope failure

Figure 7 shows the spatial distribution of the probability of slope failure computed by Eq. (1) for the *Mw* 6.8 scenario earthquake. Note that the probability of slope failure is set to be zero for the cell where the gradient is less than 10°. Although the slope gradients which shown in Fig. 4 have larger values in the eastern part of Chizu Town, the probabilities of slope failures take larger values in the western part of the town. This is because the values of PGA have larger in the western part rather than the eastern or central part of the town, as shown in Fig. 5. The probabilities of slope failure depend on the used cell size. Sakai et al. [8] used the database of slope failures in the spatial resolution of 10 m grid for developing Eq. (1). Therefore, we adapted the same spatial resolution.

4.2 Probability of node and edge failure

Figure 8 shows the spatial distribution of the probabilities of node failure. The probability of failure of each node was obtained by simply picking up the probability of slope failure corresponding to the cell that the node exists. On the other hand, Fig. 9 shows the spatial distribution of the probability of edge failure. From these figures, the roads that are likely to be closed after the scenario earthquake were identified. However,

considering the existence of alternative routes, there are still some difficulties in identifying the nodes with high isolation risk.

The probability of edge failure tends to have a higher value than that of a node failure, as is obvious from the calculation process. Furthermore, the longer the edge length is, the probability of edge failure has a higher value. As a result, for 60% of the edges, the probability of failure is greater than 0.8, while approximately 73% of the nodes have the probability of failure less than 0.01.

Note that the probabilities of node and edge failures obtained here may be overestimated. We assume that a node is completely blocked if a slope failure occurs in the cell where the node exists regardless of the magnitude of the slope failure. The same assumption is given to edge failure. If a slope failure occurs in one of the cells where the edge is placed, the edge is considered as completely blocked. However, the road may remain some transportation capacity unless the road is completely damaged.

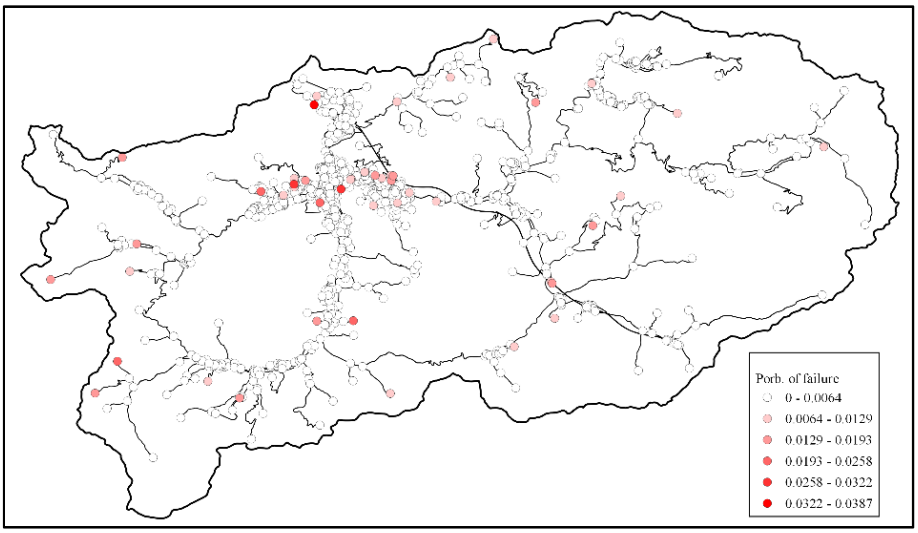

Fig. 8 – Probability of node failure

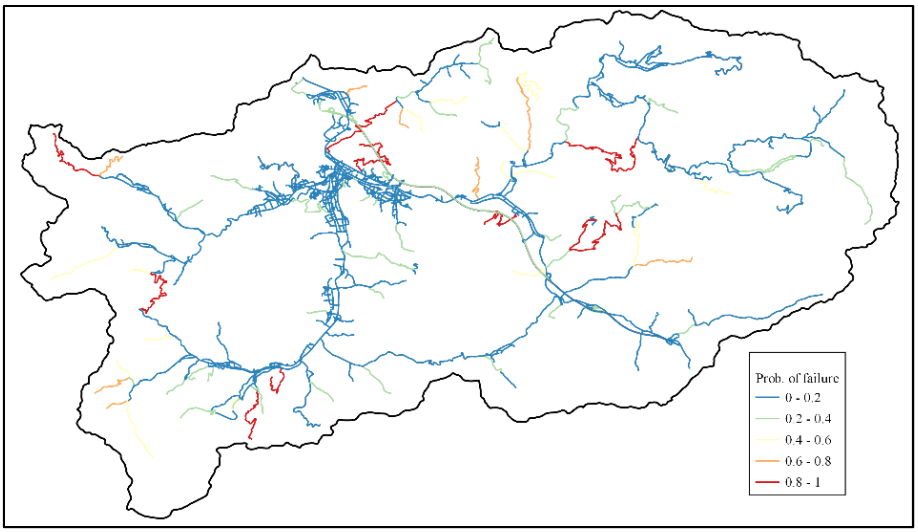

Fig. 9 – Probability of edge failure

4.3 Probability of isolation

Using the probabilities of node and edge failures shown in Figs. 8 and 9, the probability of isolation for each node was calculated by the MC method with 3,000 trials. As mentioned earlier, the probability of isolation for a node is defined as the probability of disconnection from the node to the node of the town hall. To conduct the analysis, we gave two assumptions: road blockages are caused only by slope failures, while damage to bridges, tunnels, and other structures are not considered; The available road network is limited in the town. In other words, the connections crossing the town boundary to the neighboring ones are ignored.

Figure 9 shows the spatial distribution of the probability of isolation. The nodes near the town boundary have a higher probability of isolation than the nodes in the center of town where the node of the town hall is located. Not only on the distance from the town hall node but also on the number of available paths are considered for evaluating the probability of isolation.

The authorities responsible for earthquake disaster prevention may plan the road retrofitting and emergency response base on the result. However, some of the nodes whose probabilities of isolation are relatively high may not be a residential area. In general, countermeasures should be given priority from the most populated area. Therefore, we need to consider not only the probability of isolation but also population data.

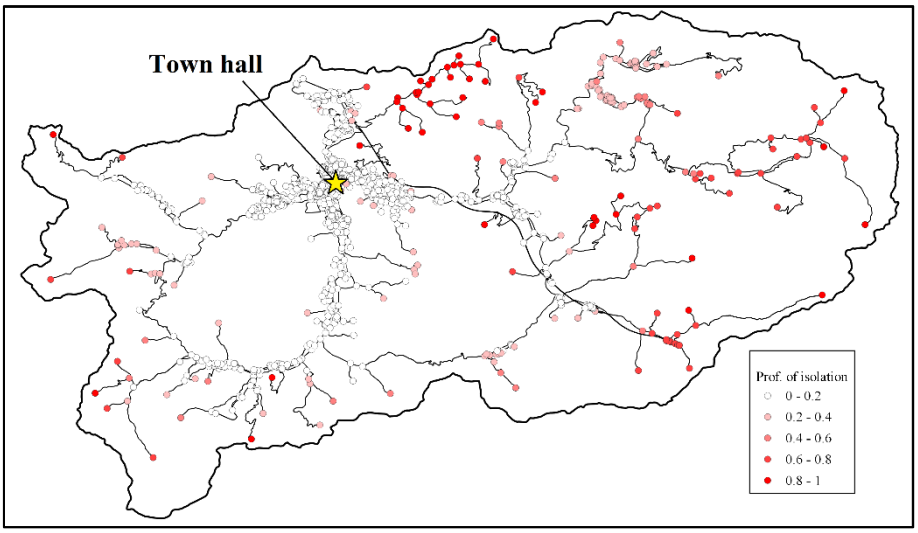

Fig. 10 – Probability of isolation

4.4 Expected number of the isolated residents

As a result, 690.28 people are expected to be isolated in the town for the given scenario earthquake. The largest expected number of the isolated residents for one ward is 103.8. Fig.11 highlights the wards that have high isolation risk.

The result provides essential information to the authorities, policymakers, and stakeholders in the town. For instance, the areas where some countermeasures to prevent isolation considering the scenario earthquake should be taken were revealed; The required stock of food and daily necessities in each ward can be estimated; The isolation riks of the town was quantified and was possible to compare with other areas. Furthermore, the effect of road retrofitting can be confirmed by evaluating the expected values of isolated people for the retrofitted road network.

There are some shortcomings of the present study, and, therefore, further studies are required. Firstly, slope failure was only involved as a cause of road blockage. Other factors, such as damage to bridges and tunnels et al., also induce road blockage. Secondly, the magnitude of slope failure is not considered. If the

magnitude of slope failure is small, some transportation capacity may remain. Ideally, the probability of road closure should be a function of the probability of occurrence of slope failure and its magnitude. Thirdly, the results depend on the spatial resolution of the data used. We need to investigate the proper spatial resolution for the analysis. Fourthly the population should be allocated to nodes more accurately. The population of each node was calculated simply by dividing the total population of the ward by the number of nodes in the same ward. We need to develop a systematic method to assign more realistic population data to nodes.

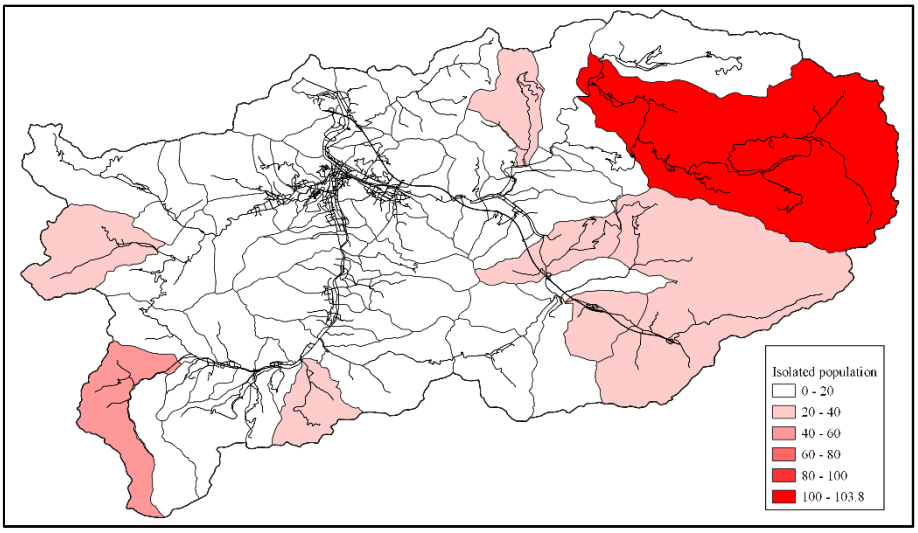

Fig. 11 – Expected number of the isolated residents

5. Conclusion

This paper has presented a methodology to analyze isolation risk for a rural town in a mountainous area considering road blockages caused by slope failures under a predefined scenario earthquake. We defined the isolation risk of residents by the expected number of the isolated residents. The reliability analysis of connectivity was utilized to calculate the probabilities of isolation for residents. We examined the isolation risk in Chizu Town, Tottori, Japan, as a case study. The scenario earthquake of *Mw* 6.8 in the Nagisan fault zone was considered. The road network in Chizu Town was modeled as a graph. After the probabilities of node and edge failures were computed, the probabilities of isolation for each node were estimated. Then the expected number of the isolated residents was evaluated for each ward in the town. The presented results enable us to know which areas in the town have higher isolation risk. Furthermore, we can discuss the effect of possible mitigation strategies quantitatively.

Acknowledgments

The road network data used in this study was obtained from OpenStreetMap. The digital elevation model published by the Geospatial Information Authority of Japan (GSI) was used. The JMA seismic intensity map for the scenario earthquake released by Japan Seismic Hazard Information Station (J-SHIS) was used. This work was supported by JSPS KAKENHI Grant Number JP17K01343.

References

[1] Loh, C.H., Lee, C.Y., Yeh, C.H. (2003): Seismic Risk Assessment of Transportation System: Evaluation Immediately After Earthquake, *Technical Council on Lifeline Earthquake Engineering Monograph*, 123–132.

[2] Chen, Y., Eguchi, R.T. (2003): Post-Earthquake Road Unblocked Reliability Estimation based on an Analysis of Randomicity of Traffic Demands and Road Capacities, *Technical Council on Lifeline Earthquake Engineering Monograph*, 916–925.

[3] Runzhou, L. (2008): Study on the Post-Earthquake Connectivity of Transportation System Network, *The14th World Conference on Earthquake Engineering*, Beijing, China.

[4] Giovinazzi, S., Nicholson, A. (2010): Transport Network Reliability in Seismic Risk Analysis and Management, *14th European Conference on Earthquake Engineering*, 933.

[5] Shoji, G., Toyota, A. (2012): Function of Emergency Road Networks During the Post-Earthquake Process of Lifeline Systems Restoration, *Journal of Disaster Research*, **7** (2), 173–183.

[6] Kermanshah, A., Derrible, S. (2016): A geographical and multi-criteria vulnerability assessment of transportation networks against extreme earthquakes, *Reliability Engineering and System Safety*, **153** 39–49.

[7] Michael-Leiba, M., Baynes, F., Scott, G., Granger, K. (2003): Regional landslide risk to the Cairns community, *Natural Hazards*, **30** (2), 233–249.

[8] Sakai, H., Okumura, M., Shiwaku, T., Kagawa, T., Hasegawa, K., Sawada, S., Tatano, Y. (2013): A fundamental study on simplified method for calculating earthquake-induced slope collapse ratio, *Journal of Japan Society of Civil Engineers, Ser. A1 (Structural Engineering & Earthquake Engineering)*, **69** (4), I_142-I_147.

[9] Fujimoto, K., Midorikawa, S. (2010): Empirical relationship between JMA instrumental seismic intensity and ground motion parameters considering the effect of earthquake magnitude, *Journal of Japan Association for Earthquake Engineering*, **10** (2), 1–11.

[10] Haklay, M., Weber, P. (2008): OpenStreet map: User-generated street maps, *IEEE Pervasive Computing*, **7** (4), 12–18.

[11] Boeing, G. (2017): OSMnx: New methods for acquiring, constructing, analyzing, and visualizing complex street networks, *Computers, Environment and Urban Systems*, **65** 126–139.

[12] Fard, N.S., Lee, T.H. (1999): Cutset enumeration of network systems with link and node failures, *Reliability Engineering and System Safety*, **65** (2), 141–146.

[13] Kobayashi, K., Yamamoto, H. (1999): New algorithm in enumerating all minimal paths in a sparse network, *Reliability Engineering and System Safety*, **65** (1), 11–15.

[14] Javanbarg, M.B., Scawthorn, C., Kiyono, J., Ono, Y. (2009): Minimal path sets seismic reliability evaluation of lifeline networks with link and node failures, *TCLEE 2009: Lifeline Earthquake Engineering in a Multihazard Environment*, **357** (May 2014), 105.

[15] Ching, J., Hsu, W.C. (2007): An efficient method for evaluating origin-destination connectivity reliability of real-world lifeline networks, *Computer-Aided Civil and Infrastructure Engineering*, **22** (8), 584–596.

[16] Li, J., He, J. (2002): A recursive decomposition algorithm for network seismic reliability evaluation, *Earthquake Engineering & Structural Dynamics*, **31** (8), 1525–1539.

[17] Fishman, G.S. (1986): A Comparison of Four Monte Carlo Methods for Estimating the Probability of s-t Connectedness, *IEEE Transactions on Reliability*, **35** (2), 145–155.

[18] Yeh, W.C. (2004): A simple MC-based algorithm for evaluating reliability of stochastic-flow network with unreliable nodes, *Reliability Engineering and System Safety*, **83** (1), 47–55.

[19] Ramirez-Marquez, J.E., Coit, D.W. (2005): A monte-carlo simulation approach for approximating multi-state two-terminal reliability, *Reliability Engineering and System Safety*, **87** (2), 253–264.

[20] Hagberg, A., Schult, D., Swart, P. (2008): Exploring Network Structure, Dynamics, and Function using NetworkX, *Proceedings of the 7th Python in Science Conference*, 11–15.

